Int. J. Electrochem. Sci., 15 **(2020)** 2470 – 2480, doi: 10.20964/2020.03.09

International Journal of ELECTROCHEMICAL SCIENCE
www.electrochemsci.org

Enhanced photocatalytic performance of $BiVO_4$ for degradation of methylene blue under LED visible light irradiation assisted by peroxymonosulfate

Shoufeng Tang[1], *Zetao Wang*[1], *Deling Yuan*[*, 1], *Yating Zhang*[1], *Jinbang Qi*[1], *Yandi Rao*[1], *Guang Lu*[4], *Bing Li*[5], *Kai Wang*[3], *Kai Yin*[2]

[1] Hebei Key Laboratory of Heavy Metal Deep-Remediation in Water and Resource Reuse, Hebei Key Laboratory of Applied Chemistry, School of Environmental and Chemical Engineering, Yanshan University, Qinhuangdao 066004, P. R. China
[2] Hunan Key Laboratory of Super Microstructure and Ultrafast Process, School of Physics and Electronics, Central South University, Changsha, 410083, P. R. China
[3] School of Electrical Engineering, Qingdao University, Qingdao, 266000, P. R. China
[4] College of Chemistry, Chemical Engineering and Environmental Engineering, Liaoning Shihua University, Fushun, Liaoning, 113001, P. R. China
[5] Department of Chemical & Materials Engineering, Faculty of Engineering, The University of Auckland, Private Bag, 92019, Auckland, New Zealand
[*]E-mail: yuandeling83@126.com

Received: 5 November 2019 / *Accepted:* 17 December 2019 / *Published:* 10 February 2020

The enhancement of $BiVO_4$ photocatalytic degradation of methylene blue (MB) through peroxymonosulfate (PMS) introduction was studied under LED light irradiation. The $BiVO_4$ catalyst was prepared by the hydrothermal method, and its physicochemical properties were characterized through various surface means. The influencing factors on the MB decolorization, such as the PMS concentration, $BiVO_4$ amount, initial solution pH value, and catalyst stability were determined. The results presented that the photocatalytic performance of $BiVO_4$ for MB removal was effectively improved after adding the PMS in the photocatalysis system. Increasing $BiVO_4$ and PMS dosages promoted the MB elimination, and the synergy process showed satisfactory MB decolorization effect from pH 4 to 10. Besides, the coupling system exhibited a good stability after the four recycles. Moreover, the reactive species were identified by radicals scavenging experiments, and the results displayed that the sulfate and hydroxyl radicals were in charge of the MB decomposition during this collaborative process.

Keywords: $BiVO_4$; Photocatalysis; LED visible light; Peroxymonosulfate; Methylene blue degradation

1. INTRODUCTION

Organic dyes is one of the most common contaminants in industrial wastewater, and their untreated discharges would cause serious harms to ecological environment and human health [1, 2]. There are numerous methods to eliminate dyes from water, such as physical [3, 4], biological [5, 6], and chemical methods [7, 8]. However, searching for a quick and efficient way to treat the dye wastewaters is still a challenge.

Advanced oxidation processes (AOPs) have attracted considerable attentions for the efficient removal of recalcitrant organic matters [9, 10]. The most common AOPs for the dye decomposition include ozonation [11], Fenton [12], electrochemical oxidation [13], persulfate activation oxidation [14, 15], and photocatalysis [16, 17]. Among them, the photocatalysis method could transform solar energy to chemical energy to decompose organics with environmental friendship and without second contamination [18, 19]. Especially the visible light photocatalytic technique is the focus of research recently [20, 21].

Monoclinic scheelite bismuth vanadate ($BiVO_4$) is a benign visible light driven semiconductor photocatalyst [22], which has the following characteristics: appropriate band gap (near 2.5 eV), non-toxic, well chemical durability, and great photocatalysis performance [23]. Nevertheless, the $BiVO_4$ application is impeded due to the low charge separation capacity and poor visible light adsorption efficiency [24]. To overcome the obstacles, modifying with nanocomposites or combining with other AOPs are the regular means to improve its use performance.

Peroxymonosulfate (PMS), as one of the persulfates, has been extensively researched in the organics oxidation under various activation means, such as ultraviolet (UV), alkali, and catalysis [25]. The activated PMS can produce strong oxidative sulfate radical ($HSO_5^-/SO_4^{\cdot-}$, 2.5–3.1 V) over a wide pH range after the peroxide bond of PMS being cleaved through the excitations of energy and electrons transfer [26]. Previous researchers found that photocatalytic activation for PMS is feasible, and the light source mainly is UV. But the visible-light photocatalytic motivation of PMS is much more desirable [27]. Furthermore, the combination of photocatalysis and PMS activation would promote charge separation in the photocatalytic system as an electron trapping agent, and then improve the light utilization of photocatalyst [28].

Additionally, the traditional photocatalysis relies mostly on xenon or high-pressure mercury lamps to produce UV or visible light. Although it provides a stable light source, it consumes too much energy and emits lots of heat [29]. Hence, the LED light source has become eye-catching in the photocatalysis with low-energy, feasible, and reliable properties in recent years [30].

To sum up, activating PMS by the LED light would be a promising way to enhance the $BiVO_4$ photocatalytic performance. Therefore, a $BiVO_4$ catalyst was prepared and added in to the visible light photocatalysis system with PMS simultaneously serving for the methylene blue (MB) degradation in this study. The MB decolorization activity in this synergetic system was compared with the PMS and photocatalysis alone systems. The influencing factors on the MB removal, such as PMS concentration, $BiVO_4$ amount, initial pH value, and catalyst stability were investigated in the photocatalytic activation of PMS coupling processes. Lastly, the possible catalytic mechanism was proposed based on the radical scavenger test.

2. EXPERIMENTAL

MB, PMS ($KHSO_5 \cdot 0.5KHSO_4 \cdot 0.5K_2SO_4$), bismuth nitrate pentahydrate ($Bi(NO_3)_3 \cdot 5H_2O$), ammonium vanadate (NH_4VO_3), nitric acid (HNO_3), sodium hydroxide (NaOH), sodium sulfate (Na_2SO_4), sodium dodecyl benzene sulfonate (SDBS), ammonium oxalate (AO), methanol (MA), tert-butanol (TBA), and p-benzoquinone (BQ) were of analytical grade and supplied from Sinopharm Chemical Reagent Company. All materials were employed directly without being further purified. Deionized (DI) water was applied throughout the research.

The $BiVO_4$ was prepared by the hydrothermal method. 2.45 g $Bi(NO_3)_3 \cdot 5H_2O$ and 0.58 g NH_4VO_3 were dissolved into 10 mL 4 mol/L HNO_3 solution and 2 mol/L NaOH solution, respectively. Then, 0.25 g SDBS was added into both of above solutions under vigorous stirring. After stirring for 0.5 h, the two solutions were mixed to obtain a bisque solution. 2 mol/L NaOH was added to adjust the pH value to 7, and then the mixture was continues stirring for 0.5 h. After that, the suspension was transferred into a 50 mL Teflon-lined stainless-steel autoclave, which was kept in an oven at 200℃ for 3 h. After the autoclave was cooled to room temperature, the resultant vivid yellow sample was separated by centrifugation and washed with DI water and ethanol several times, and then dried at 100℃ for 4 h.

The $BiVO_4$ was characterized by X-ray diffraction (XRD, D-max-2500), scanning electron microscopy (SEM, SUPRA55), energy-dispersive X-ray spectroscopy (EDS), and X-ray photoelectron spectroscopy (XPS, Thermo Scientific ESCA Lab 250). XRD patterns were carried out with Cu Kα radiation (l = 0.15418 nm), which operated at 40 kV and 30 mA, and the scan rate is 5° min^{-1}. The SEM was a field-emission SEM equipped with an EDS for the elemental analysis. XPS investigation was recorded with a monochromatic Al Kα as the X-ray source and hemispherical analyzer.

The photocatalytic activity of $BiVO_4$ was determined by the decolorization of MB under a LED lamp (GRF30, 30 W, 400~780 nm). A certain dose of $BiVO_4$ was introduced in 100 mL MB. Before illumination, 10 min dark adsorption with stir was to achieve the adsorption-desorption equilibrium. Then the determined amount of PMS was added to begin the synergistic reaction. The residual concentration of MB with time was determined by an UV spectrophotometry (SP-725) at 664 nm. Besides, the mineralization of MB was evaluated by the COD and TOC removal. The COD was measured by a COD rapid tester (DRB 200). The total organic carbon (TOC) was analyzed through a TOC analyzer (Shimadzu-VCPH).

3. RESULTS AND DISCUSSION

The crystallographic structure of $BiVO_4$ was identified by XRD as displayed in Figure 1a. It is obvious to see that the diffraction peaks for the $BiVO_4$ could accord with the standard maps of the pure monoclinic phase of bismuth vanadate [31].

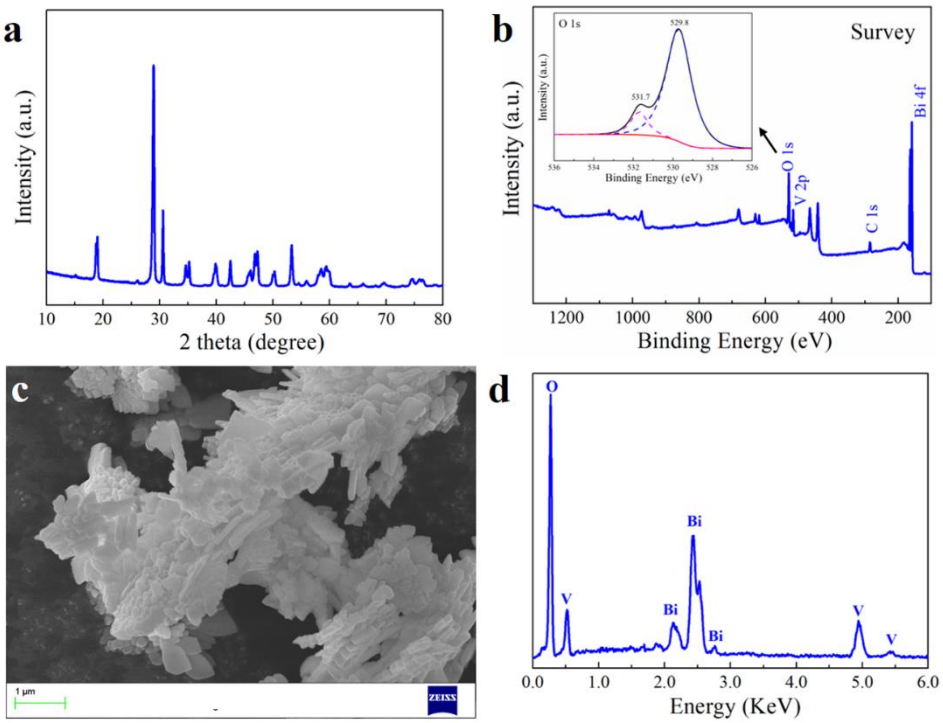

Figure 1. $BiVO_4$ characterization of XRD (a), XPS (b), SEM (c), and EDS (d).

As presented in Figure 1b, the survey XPS spectrum of $BiVO_4$ was clearly revealed. The peaks at 164.0 and 158.6 eV of $BiVO_4$ belonged to Bi $4f_{5/2}$ and Bi $4f_{7/2}$, respectively. The C 1s peaks could be due to the carbonaceous compounds in the air adsorbed on the catalyst surface [32, 33]. As seen in the illustration of Figure 1b, the peaks at 529.8 and 531.7 eV in $BiVO_4$ were attributed to the crystal oxygen (O 1s) in the $Bi_2O_2^{2+}$ lattice, which represented the formation of the V-O bond [34, 35]. Those results demonstrated that Bi^{3+}, V^{5+}, and O^{2-} were observed in the fabricated $BiVO_4$ sample. The SEM image (Figure 1c) indicated that the prepared $BiVO_4$ displayed a typical sheet-like morphologies in the range of 200-500 nm. The EDS patterns (Figure 1d) corroborated that the representative peaks of Bi, V, and O elements were detected. Above results prove that $BiVO_4$ nanoparticles were successfully synthesized.

The MB decolorizations in different system are presented in Figure 2a. The experimental conditions were as follows: the initial concentration of MB 5 mg L^{-1}, PMS dosage 1 mmol L^{-1}, $BiVO_4$ dosage 0.2 g L^{-1}, and initial solution pH 6. It can be observed that $BiVO_4$ itself had a weak adsorption capacity for the MB, and almost no decolorization effect on the MB under LED light. The removal ratio of MB by PMS alone was 46%, while the decolorization only increased to 50% after adding the visible light irradiation, indicating that visible light has almost no activation effect on PMS. The MB degradation was just reached 51% under the $BiVO_4$ system added PMS without light, which could be due to the common effects of $BiVO_4$ adsorption and PMS oxidation. However, under the irradiation of visible light, 99% MB was decolorized in the presence of $BiVO_4$ and PMS, which demonstrated that MB degradation over $BiVO_4$ catalysts was significantly promoted after adding PMS into the photocatalytic process ($BiVO_4$ + PMS +Vis system). The MB removal kinetics trials satisfied the first order kinetics, as displayed in Figure 2b. The kinetics change trends of different systems were consistent with those in the

MB decolorization processes. The kinetic constant of MB decolorization for the $BiVO_4$ + PMS +Vis process was 0.279 min^{-1}, which was higher than that of the sole $BiVO_4$ photocatalysis (0.0745 min^{-1}) and sole PMS (0.0964 min^{-1}) processes, respectively.

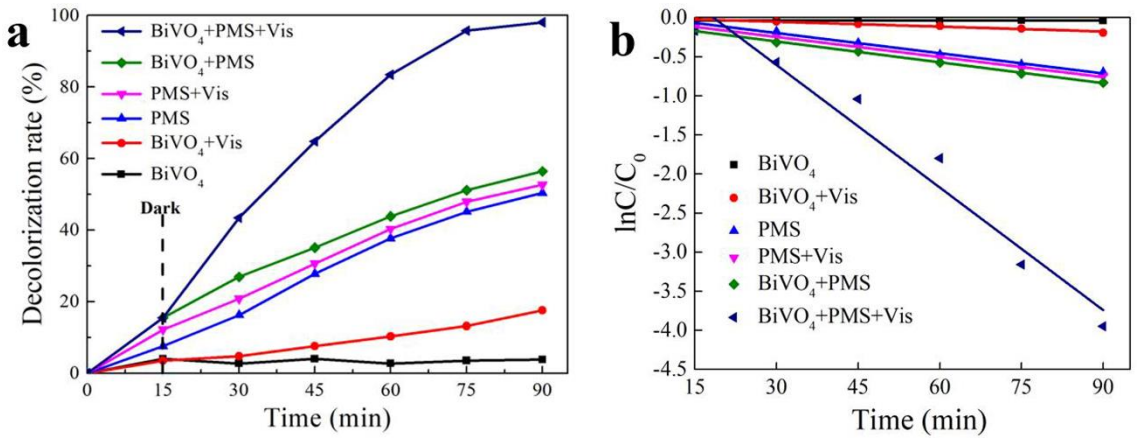

Figure 2. MB degradation with different systems(a) and corresponding kinetic curves (b).

Figure 3a shows the effect of different PMS dosages on the MB decolorization in the $BiVO_4$ + PMS +Vis system. The experimental conditions were the following: MB initial concentration 5 mg L^{-1}, initial pH 5.9, and $BiVO_4$ dose 0.2 g L^{-1}. In the dark reaction, the MB decolorization was increased with the increasing PMS dosage. This is due to PMS is a strong oxidant itself, the more PMS added, the more dye molecules are decomposed in the synergistic system. After turning on the light source, expect for the excess PMS amount 5.0 mmol L^{-1}, the MB removals were all accelerated obviously. More active species ($SO_4^{\cdot-}$ and ·OH) would be generated in the photocatalytic coupling process with the increasing PMS, improving the decolorization effect. Besides, the PMS could act the photogenerated electron capture agent, the augment of PMS dose would decrease the recombination of photogenerated carriers [2]. Since the final degradation effects of PMS dose 1 and 5 mmol L^{-1} were the same, 1 mmol L^{-1} was selected as the optimal PMS dosage from the cost reason.

Figure 3b displays the effect of different amounts of $BiVO_4$ on the decolorization effect during the $BiVO_4$ + PMS +Vis process. The test parameters were as follows: MB initial amount 5 mg L^{-1}, beginning pH 5.9, and PMS dose 1 mmol L^{-1}. During the dark stage, the decolorization effect of MB was not affected by the change of the $BiVO_4$ amount, which could be attributed to the small specific surface area and poor adsorption performance for the $BiVO_4$. At this point, the PMS activation plays a major role for the MB decomposition. Under the LED irradiation, the MB decolorizations were promoted as the dosage of $BiVO_4$ increased. It is generally believed that more photocatalyst were introduced into this system, more photocatalytic reactions would be generated, enhancing the PMS activation and the MB removal. After the comprehensive consideration, 0.2 g L^{-1} was chosen as the suitable $BiVO_4$ amount in the next experiments.

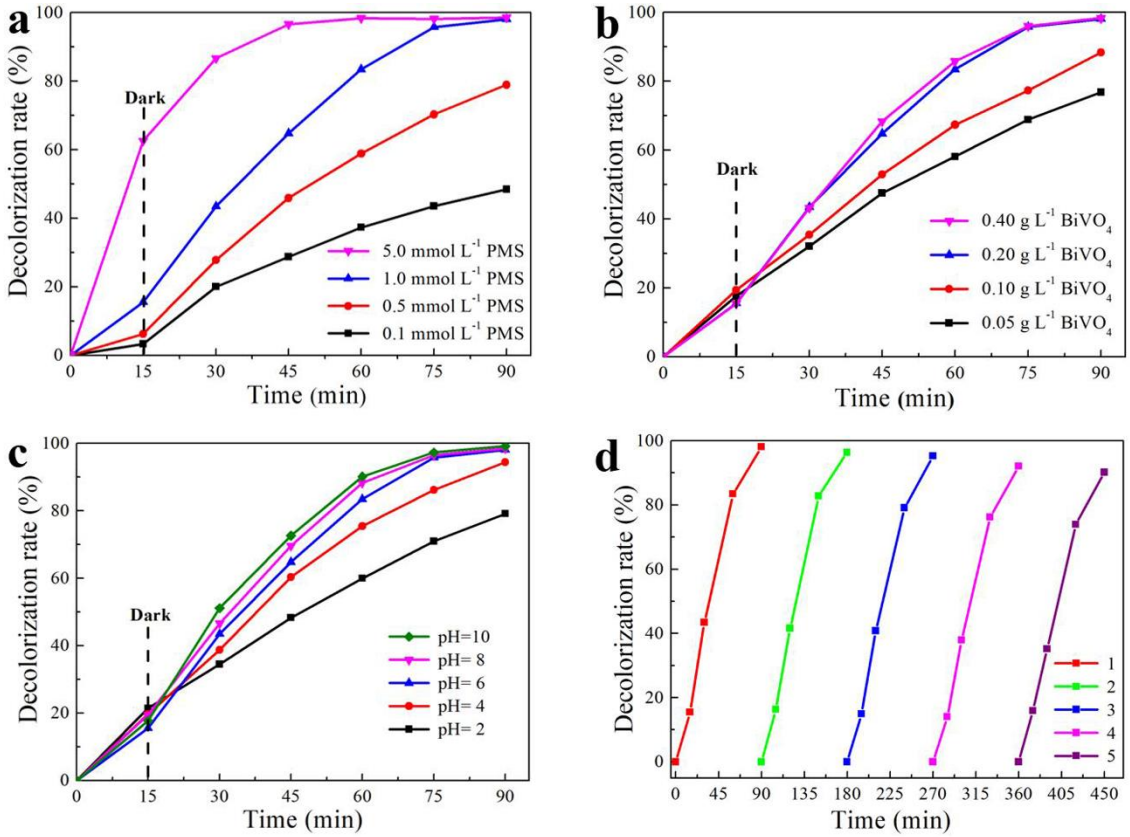

Figure 3. Effect of PMS amount (a), $BiVO_4$ dosage (b), and initial solution pH (c) on MB decolorization. Cycle photocatalytic tests for MB decolorization (d).

Figure 3c illustrates the impact of initial pH on the decolorization of MB for the $BiVO_4$ + PMS +Vis. The operation conditions were as follows: MB concentration 5 mg L^{-1}, PMS dosage 1 mmol L^{-1}, and $BiVO_4$ dosage 0.2 g L^{-1}. The initial pH change had little effect on the degradation of MB in the dark reaction. After turning on the light source, it is apparent that the decolorization effects under neutral and alkaline conditions were better than that in the acidic environment. Under alkaline conditions, HSO_5^- is more easily to be activated, producing more $\cdot SO_4^- \cdot$, promoting the dye decolorization efficiency [14]. Moreover, the $BiVO_4$ and PMS photocatalytic system broadened the range of reaction pH for the individual $BiVO_4$ and PMS, which would be conducive to the real application for this synergy process.

Figure 3d depicts the stability test results of the $BiVO_4$ + PMS +Vis process. The MB decolorization rate of the synergistic system still reached 90% after five repeated cycles. These results indicated that the $BiVO_4$ could maintain the high catalytic activity after multiple reactions in the synergetic system, and thus continuously activate PMS. However, the catalyst would be deactivated and gradually lost during the photocatalysis and recovery step, respectively, leading to the decreasing of photocatalytic performance.

The further degradation and mineralization effects for the MB were determined by the COD and TOC analyses, and the results are presented in Figure 4a and 4b, respectively. The COD removal in the $BiVO_4$ + PMS +Vis was 40%, which was significantly higher than that in the systems of $BiVO_4$ alone (9%) and PMS alone (27%) under visible light irradiation. On the other side, the TOC removal for the synergy process reached 31%, which was also obviously improved than the $BiVO_4$ + Vis (5%) and PMS

+ Vis (16%) processes. It can be concluded that the synergistic effect of the $BiVO_4$ + PMS +Vis not only improved the degradation of organic matter, but also enhanced its mineralization ability. However, when the MB was attacked by the free radicals generated in the coupling system, some degradation intermediates were formed by a series of decomposition reactions, such as demethylation and dehydrogenation reactions [36-38]. These byproducts were hard to be mineralized completely.

Moreover, the UV-visible full-spectral scan was performed to confirm the MB decomposition in the $BiVO_4$ + PMS +Vis system, and the experimental conditions were as follows: MB 5 mg L^{-1}, PMS dosage 1 $mmol^{-1}$, $BiVO_4$ dosage 0.2 g L^{-1}, and initial pH 6. As observed in Figure 4c, the maximum absorption peak intensity at 664 nm decreased with the reaction proceeding, indicating that the chromophoric group of the MB molecular structure was completely destroyed [39, 40]. Meanwhile, the blue MB solution also discolored to colorless as seen in the illustration of Figure 4c.

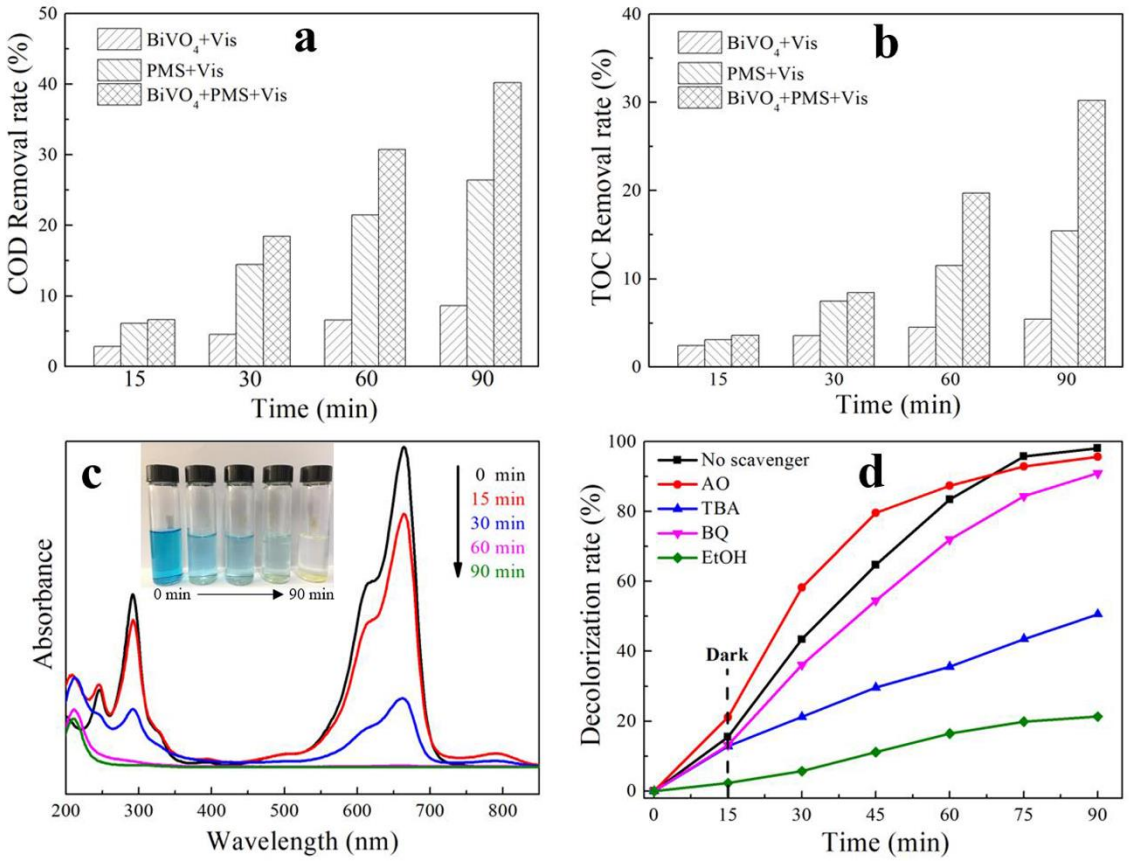

Figure 4. COD (a) and TOC (b) removals of MB in different systems. (c) UV-Vis spectra analysis of MB in $BiVO_4$ + PMS +Vis system. (d) Effect of radical scavengers on MB decolorization for $BiVO_4$ + PMS +Vis process.

Figure 4d shows the free radical masking experiment of the $BiVO_4$ + PMS +Vis system under above optimized reaction conditions. In this experiment, AO, BQ, TBA, and EtOH were used as the inhibitors of h^+, $\cdot O_2^-$, $\cdot OH$, and $\cdot SO_4^-$, respectively. After the addition of BQ and TBA, the degradation

was not significantly suppressed at the end of the dark reaction. However, there was almost no decolorization effect during the dark reaction as adding EtOH. Above results indicated that the nonradical function of PMS played the major role in the dark reaction process rather than other active radicals. When the LED light was turned on, a small inhibitory effect on the MB decolorization was represented under the introduction of BQ, and the final removal rate reached 90%, proving that the $\cdot O_2^-$ was not the main active substance in this system. Nevertheless, the decolorization efficiency only achieved 49% after adding TBA, which demonstrated that ·OH acted a certain role. Furthermore, when EtOH was used as the quenching agent, the MB degradation sharply decreased to 19% after 90 min treatment, this result indicated that $SO_4^-\cdot$ could be the most significant free radicals in the synergetic process. In addition, the removal rate was found to be accelerated after adding AO, this could be due to the combination of AO and h^+ would promote the e^- production on the $BiVO_4$, which could further activate PMS and then produce more reactive radicals.

Hence, it can be concluded that the action order of the reactive species in the $BiVO_4$ + PMS +Vis system was $SO_4^-\cdot > \cdot OH > \cdot O_2^- > h^+$. Because the conduction band position of $BiVO_4$ is not conducive to the generation of $\cdot O_2^-$, and the PMS captures a large amount of e^-, which would inhibit the O_2^- formation [41, 42]. Besides, due to the higher valence band position of $BiVO_4$, h^+ can react with OH^- to produce more ·OH, promoting the degradation of MB [15, 43, 44]. $SO_4^-\cdot$ plays a vital role in the coupling process, which is not only the highly oxidative radical involved in the decomposition of MB, but also participate the ·OH generation in water, thereby improving the decolorization efficiency. Moreover, ·OH could be generated by the reactions of OH^- with h^+ and $SO_4^-\cdot$, respectively, so the synergy effect would be prominent in the alkaline condition as previous pH control tests [45, 46]. The related reaction equations were listed as follows:

$$BiVO_4 + h\nu \rightarrow h^+ + e^- \quad (1)$$

$$e^- + O_2 \rightarrow \cdot O_2^- \quad (2)$$

$$h^+ + OH^- \rightarrow \cdot OH \quad (3)$$

$$HSO_5^- + e^- \rightarrow SO_4^-\cdot + OH^- \quad (4)$$

$$HSO_5^- + h^+ \rightarrow SO_5^-\cdot + H^+ \quad (5)$$

$$HSO_5^- + \cdot OH \rightarrow SO_5^-\cdot + H_2O \quad (6)$$

$$2SO_5^-\cdot \rightarrow 2SO_4^-\cdot + O_2 \quad (7)$$

$$SO_4^-\cdot + OH^- \rightarrow \cdot OH + SO_4^{2-} \quad (8)$$

$$SO_4^-\cdot + SO_4^-\cdot \rightarrow S_2O_8^{2-} \quad (9)$$

$$S_2O_8^{2-} + OH^- \rightarrow SO_4^{2-} + \cdot OH \quad (10)$$

$$SO_4^-\cdot / \cdot OH / \cdot O_2^- / h^+ + MB \rightarrow \text{degraded products} \quad (11)$$

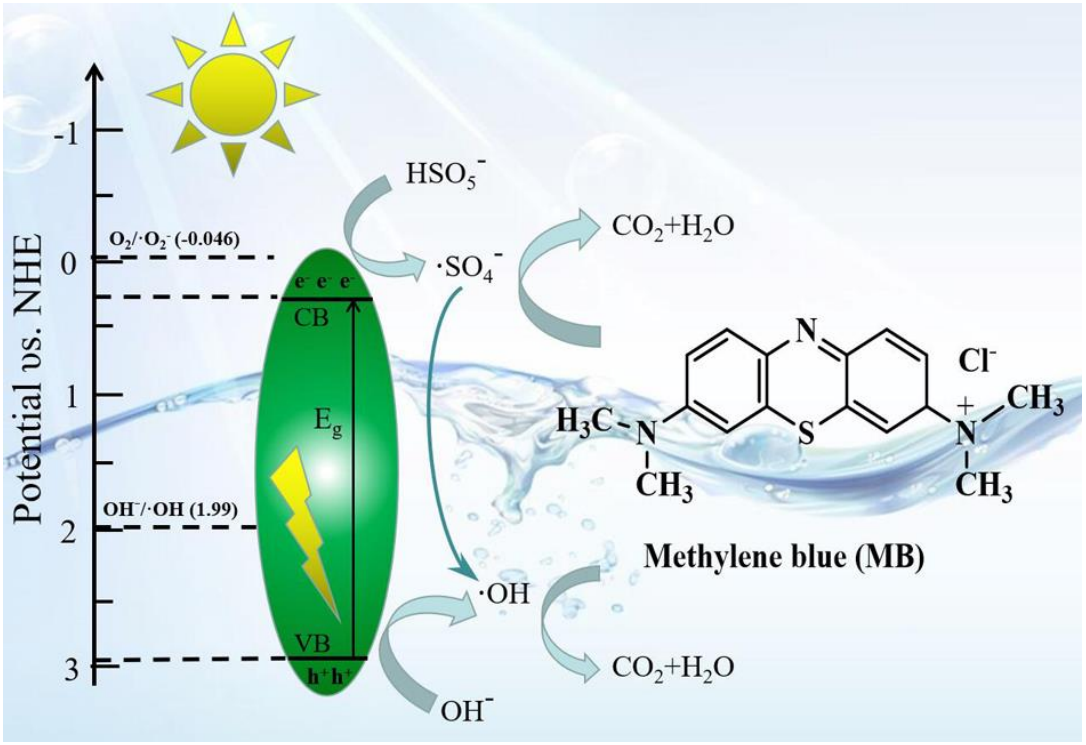

Figure 5. Possible photocatalytic mechanism of synergistic system.

Figure 5 displays the migration path of photogenerated carriers and the generation of free radicals in the $BiVO_4$ + PMS +Vis system. Under the irradiation of LED light, the addition of PMS improved the separation of photo-generated carriers of $BiVO_4$, then inhibited the recombination of photo-generated carriers, and thus produced more e^- and h^+. On the one hand, e^- could be trapped by PMS, and then activate PMS to generate $SO_4^-\cdot$, which enhanced the catalytic activity of $BiVO_4$. On the other hand, a small number of e^- would react with O_2 to form $\cdot O_2^-$, which could inhibit the recombination of carriers and then benefit the ·OH generation through the reaction of h^+ and OH^-. So, the MB was degraded and mineralized to CO_2 and H_2O by above strong oxidative radicals generated in the synergistic process.

4. CONCLUSIONS

In this work, the photocatalytic performance of $BiVO_4$ nanosheets for the MB degradation was effectively promoted with the introduction of PMS under LED visible light irradiation. The first order rate constants of the MB removal were enhanced to 0.279 min^{-1} for the $BiVO_4$ + PMS +Vis system from 0.0745 min^{-1} and 0.0964 min^{-1} for the sole $BiVO_4$ photocatalysis and PMS oxidation alone, respectively. Increased the $BiVO_4$ dose and PMS amount could both improve the synergetic activity for the MB degradation. The $BiVO_4$/PMS coupling process could broaden the pH reaction ranges, which presented fair decolorization efficiencies from pH 4 to 10. The synergy process exhibited a good stability in the four recycle tests. The $BiVO_4$ + PMS +Vis process displayed the better COD and TOC removal ratios than the $BiVO_4$ + Vis and PMS + Vis systems, respectively. The $SO_4^-\cdot$ and ·OH radicals were identified as the main oxidative radicals for the MB degradation. The added PMS could trap e- and enhance the

separation of photogenerated hole electron pairs, which can significantly the photocatalytic performance of $BiVO_4$ under the LED light irradiation.

ACKNOWLEDGMENTS
This study is supported by the National Natural Science Foundation of China (Project Nos. 51908485 and 51608468), the China Postdoctoral Science Foundation (Project No. 2019T120194), and the University Science and Technology Program Project of Hebei Provincial Department of Education (Project No. QN2018258).

References

1. J. Yin, F. Zhan, T. Jiao, H. Deng, G. Zou, Z. Bai, Q. Zhang, and Q. Peng, *Chin. Chem. Lett.*, (2019) DOI: 10.1016/j.cclet.2019.08.047.
2. N. Li, S. Tang, Y. Rao, J. Qi, P. Wang, Y. Jiang, H. Huang, J. Gu, and D. Yuan, *Electrochim. Acta*, 270 (2018) 330-338.
3. H. Chen, S. Zhang, Z. Zhao, M. Liu, and Q. Zhang, *Prog. Chem.*, 31 (2019) 571-579.
4. Y. Han, Q. Zhang, L. Wu, *Desalination*, 477 (2020) 114270.
5. C. Duan, F. Li, M. Yang, H. Zhang, Y. Wu, and H. Xi, *Ind. Eng. Chem. Res.*, 57 (2018) 15385-15394.
6. Q. Zhang, S. Bolisetty, Y. Cao, S. Handschin, J. Adamcik, Q. Peng, and R. Mezzenga, *Angew. Chem. Int. Ed.*, 58 (2019) 6012-6016.
7. Y. He, R. Wang, T. Jiao, X. Yan, M. Wang, L. Zhang, Z. Bai, Q. Zhang, and Q. Peng, *ACS Sustain. Chem. Eng.*, 7 (2019) 10888-10899.
8. N. Jiang, Y. Zhao, C. Qiu, K. Shang, N. Lu, J. Li, Y. Wu, and Y. Zhang, *Appl. Catal. B.*, 259 (2019) 118061.
9. D. Yuan, C. Zhang, S. Tang, X. Li, J. Tang, Y. Rao, Z. Wang, and Q. Zhang, *Water Res.*, 163 (2019) 114861.
10. B. Li, I.A. Udugama, S.S. Mansouri, W. Yu, S. Baroutian, K.V. Gernaey, and B.R. Young, *J. Clean. Prod.*, 229 (2019) 1342-1354.
11. Z. Wang, Q. Sun, D. Wang, Z. Hong, Z. Qu, and X. Li, *Sep. Purif. Technol.*, 209 (2019) 1016-1026.
12. B. Li, I. Boiarkina, W. Yu, and B. Young, *Environ. Sci. Pollut. Res.*, 26 (2019) 3954-3964.
13. J. Li, B. Li, H. Huang, X. Lv, N. Zhao, G. Guo, and D. Zhang, *Sci. Total Environ.*, 687 (2019) 460-469.
14. N. Li, S. Tang, Y. Rao, J. Qi, Q. Zhang, and D. Yuan, *Electrochim. Acta*, 298 (2019) 59-69.
15. X. Li, S. Tang, D. Yuan, J. Tang, C. Zhang, N. Li, and Y. Rao, *Ecotox. Environ. Safe.*, 177 (2019) 77-85.
16. D. Yuan, M. Sun, S. Tang, Y. Zhang, Z. Wang, J. Qi, Y. Rao, and Q. Zhang, *Chin. Chem. Lett.*, (2019) DOI: 10.1016/j.cclet.2019.09.051.
17. J. Ke, M. Adnan Younis, Y. Kong, H. Zhou, J. Liu, L. Lei, and Y. Hou, *Nano-Micro Lett.*, 10 (2018).
18. T. Zhang, X. Li, Q. Zhao, and Y. Rao, *Sustain. Cities Soc.,* 51 (2019) 101714.
19. H. Zhou, Z. Wen, J. Liu, J. Ke, X. Duan, and S. Wang, *Appl. Catal. B.*, 242 (2019) 76-84.
20. T. Zhang, Y. Liu, Y. Rao, X. Li, D. Yuan, S. Tang, and Q. Zhao, *Chem. Eng. J.*, (2019) DOI: 10.1016/j.cej.2019.123350.
21. J. Liu, J. Zhang, D. Wang, D. Li, J. Ke, S. Wang, S. Liu, H. Xiao, and R. Wang, *ACS Sustain. Chem. Eng.*, 7 (2019) 12428-12438.
22. B. Zhang, L. Wang, Y. Zhang, Y. Ding, and Y. Bi, *Angew. Chem. Int. Ed.*, 130 (2018) 2270-2274.
23. Y. Lu, Y. Chu, W. Zheng, M. Huo, H. Huo, J. Qu, H. Yu, and Y. Zhao, *Electrochim. Acta*, 320

(2019) 134617.
24. Y. Liu, J. Kong, J. Yuan, W. Zhao, X. Zhu, C. Sun, and J. Xie, *Chem. Eng. J.*, 331 (2018) 242-254.
25. I.A. Ike, K.G. Linden, J.D. Orbell, and M. Duke, *Chem. Eng. J.*, 338 (2018) 651-669.
26. J. Yang, X. Liu, D. Wang, Q. Xu, Q. Yang, G. Zeng, X. Li, Y. Liu, J. Gong, J. Ye, and H. Li, *Water Res.*, 148 (2019) 239-249.
27. L. Dong, T. Xu, W. Chen, and W. Lu, *Chem. Eng. J.*, 357 (2019) 198-208.
28. Y. Hu, Z. Li, J. Yang, and H. Zhu, *Chem. Eng. J.*, 360 (2019) 200-211.
29. A. Abdelhaleem, W. Chu, *Chem. Eng. J.*, 338 (2018) 411-421.
30. Y. Gao, Z. Zhang, S. Li, J. Liu, L. Yao, Y. Li, and H. Zhang, *Appl. Catal. B.*, 185 (2016) 22-30.
31. B. Gao, L. Liu, J. Liu, and F. Yang, *Appl. Catal. B.*, 129 (2013) 89-97.
32. M. Zhu, Z. Sun, M. Fujitsuka, and T. Majima, *Angew. Chem. Int. Ed.*, 130 (2018) 2182-2186.
33. G. Xia, C. Li, K. Wang, and L. Li, *Sci. Adv. Mater.*, 11 (2019) 1079-1086.
34. B. Liu, Z. Li, S. Xu, X. Ren, D. Han, and D. Lu, *J. Phys. Chem. Solids*, 75 (2014) 977-983.
35. H. Xie, J. Zhang, D. Wang, J. Liu, L. Wang, and H. Xiao, *Appl. Surf. Sci.*, (2019) 144456.
36. X. Zhao, Q. An, Z. Xiao, S. Zhai, and Z. Shi, *Chinese J. Catal.*, 39 (2018) 1842-1853.
37. S. Tang, X. Li, C. Zhang, Y. Liu, W. Zhang, and D. Yuan, *Plasma Sci. Technol.*, 21 (2019) 25504.
38. S. Tang, D. Yuan, Y. Rao, M. Li, G. Shi, J. Gu, and T. Zhang, *J. Hazard. Mater.*, 366 (2019) 669-676.
39. Z. Jia, X. Duan, W. Zhang, W. Wang, H. Sun, S. Wang, and L. Zhang, *Sci. Rep.-UK*, 6 (2016).
40. S. Yang, K. Yin, J. Wu, Z. Wu, D. Chu, J. He, and J. Duan, *Nanoscale*, 11 (2019) 17607-17614.
41. L. Xia, J. Bai, J. Li, Q. Zeng, X. Li, and B. Zhou, *Appl. Catal. B.*, 183 (2016) 224-230.
42. K. Wang, L. Li, Y. Lan, P. Dong, and G. Xia, *Math. Probl. Eng.*, (2019) DOI: 10.1155/2019/2614327.
43. Y. Zhou, Y. Huang, J. Pang, and K. Wang, *J. Power Sources*, 440 (2019) 227149.
44. H. Li, S. Guo, K. Shin, M.S. Wong, and G. Henkelman, *ACS Catal.*, 9 (2019) 7957-7966.
45. S. Tang, N. Li, D. Yuan, J. Tang, X. Li, C. Zhang, and Y. Rao, *Chemosphere*, 234 (2019) 658-667.
46. Y. Zhou, Y. Wang, K. Wang, L. Kang, F. Peng, L. Wang, and J. Pang, *Appl. Energ.*, 260 (2020) 114169.